



CORRECTION OF THE OXYGEN INTERFERENCE WITH UV SPECTROSCOPIC (DOAS) MEASUREMENTS OF MONOCYCLIC AROMATIC HYDROCARBONS IN THE ATMOSPHERE

R. VOLKAMER,* T. ETZKORN, A. GEYER and U. PLATT

Institut fuer Umweltpophysik, Im Neuenheimer Feld 366, D-69120 Heidelberg, Germany

(First received 15 July 1997 and in final form 10 February 1998. Published August 1998)

Abstract—The measurement of monocyclic aromatic hydrocarbons by Differential Optical Absorption Spectroscopy (DOAS) and Differential Absorption LIDAR (DIAL) in the atmosphere suffers from interference by the three forbidden Herzberg band systems of O₂ and a fourth band system due to the dimers O₂–O₂ and O₂–N₂ at wavelengths below 287 nm. Due to the lack of reference spectra in digital form, until now the oxygen absorptions were difficult to eliminate from atmospheric absorption spectra. In this work, reference spectra of the Herzberg bands of oxygen are presented, that allow to eliminate this oxygen interference for practical purposes. Two sets of oxygen reference spectra were recorded between 240 and 290 nm with spectral resolutions of 0.15 nm (FWHM) and 0.05 nm. Spectra were taken at 240 and 720 m absorption path lengths in several mixtures of oxygen and nitrogen from 10% O₂/90% N₂ to 100% pure O₂ at atmospheric pressure (O₂ column densities from 6×10^{22} to 1.8×10^{24} molecules cm⁻²). At the resolution of the measurements, the rotational structure of the Herzberg I band Q-branches is not resolved. Therefore, saturation effects of individual transitions of the Herzberg I bands can cause the observed band shape to vary with the column density of oxygen. This apparent deviation from Lambert Beer's law can lead to problems with the oxygen correction of atmospheric DOAS measurements. In the practical application of the oxygen reference spectra, additional problems arise, because the ratio of molecular absorption in the Herzberg bands and dimer absorption changes when the partial pressure of oxygen is varied. Even though this effect is reduced due to the presence of N₂ it needs to be accounted for, if the spectra are applied to atmospheric measurements. Solutions to these problems are discussed and demonstrated together with methods to optimize DOAS measurements of aromatic hydrocarbons. As sample application the oxygen reference spectra were used to correct DOAS measurements of monocyclic aromatic hydrocarbons carried out in the urban air of Heidelberg. Simultaneous time series of mixing ratios are presented for benzene, toluene, *p*-xylene, *m*-xylene and phenol. Mean concentrations were found to be 1.8, 2.5, 0.8, 1.2 ppb and 77 ppt, respectively. The spectra are available in digital form from the authors upon e-mail request. © 1998 Elsevier Science Ltd. All rights reserved

Key word index: Herzberg bands, oxygen, DOAS, monocyclic aromatic hydrocarbons, phenol, atmosphere.

1. INTRODUCTION

1.1. Why measure monocyclic aromatic hydrocarbons in the atmosphere?

Aromatic hydrocarbons represent an important fraction (about 30 % (w/w) in urban air) of all non-methane hydrocarbons (NMHCs) (Ioffe *et al.*, 1979; Becker, 1994). This fraction is nowadays increasing, because larger amounts of aromatics are added to presently used fuel. Even in rural areas, monocyclic aromatic hydrocarbons can contribute about 10% of the NMHCs (Nutmagal and Cronn, 1985).

Monocyclic aromatic hydrocarbons contribute to urban air pollution in four ways: First, they are in part toxic (e.g. phenol, isomers of cresol) and carcinogenic (i.e. benzene). Second, due to their high reactivity towards the OH-radical (Atkinson, 1994) they undergo photochemical oxidation and thereby promote photo-oxidant formation. Even though these mechanisms are not understood in detail till now, model calculations indicate that daytime oxidation of aromatics leads to the formation of up to 40% of the photooxidants formed from VOCs (Derwent *et al.*, 1996). Additionally, OH-substituted aromatic (phenolic) compounds like phenol and cresol-isomers are highly reactive towards the NO₃-radical. Even the low NO₃ concentrations during daytime (around 0.1 ppt) might be of importance for their daytime degradation. Third, NO₃ reactions with aromatic

* Author to whom correspondence should be addressed. Now at: CEAM, ES-46980 Paterna, Valencia, Spain. E-mail: volkamer@ceam.es

species, i.e. phenolic compounds initiate their oxidation at nighttime since the NO_3 levels at night exceed the daytime concentrations by about three orders of magnitude. NO_3 radical attack on VOCs leads to the formation of RO_2 radicals, which directly contribute to the oxidation capacity of the nighttime atmosphere (Platt *et al.*, 1990) and indirectly promote higher radical and ozone formation during the day. Fourth, photochemical degradation products from aromatic hydrocarbons are likely to be an important aerosol source in urban air (Odum *et al.*, 1997).

Overall aromatic species are a potential risk for human health and promote photochemical smog in the urban atmosphere.

1.2. Sources of monocyclic aromatic hydrocarbons

Major sources of monocyclic aromatic hydrocarbons are linked to anthropogenic activity. In urban air, cars are the dominant source for benzene, toluene and the isomers of xylene (BTX). These aromatics are added to fuel and are emitted to the urban atmosphere as part of automobile exhaust (Westerholm *et al.*, 1992). In recent years higher amounts of aromatics are being added as a lead substitute and their urban atmospheric concentration has increased considerably (Perry and Gee, 1994). Additional BTX sources are gasoline evaporation and spillage, fuelwood utilisation (Piccot *et al.*, 1992), emission during chemical manufacturing (e.g. solvent use, refuse disposal) (Eitzer, 1995) as well as household chemicals (Sack *et al.*, 1992).

In rural areas, an important contribution to the aromatic budget is transport from polluted and industrialized regions (Penkett, 1993). Natural sources of aromatic compounds include biomass burning (Black *et al.*, 1994; Eyde and Richards, 1991), volcanic eruptions (Isidorov *et al.*, 1990) as well as the biogenic production in sediments (Hunt *et al.*, 1980), seawater and lakes (Juettner and Henatsch, 1986).

1.3. Measurement techniques for aromatic hydrocarbons in the atmosphere

With aromatic hydrocarbons gaining importance for atmospheric chemistry a number of measurement techniques has been developed for their detection. Table 1 summarizes these methods and gives detectable aromatic compounds as well as respective time resolution and approximate detection limits. To date, the most common method for measuring aromatic VOCs is the combination of gas chromatography (GC) with flame-ionisation detection (FID), photoionization detection (PID) or mass-spectrometry (MS). The major advantage of GC techniques are low detection limits (below 2 ppt) for a large number of aromatics (and other VOCs) (Dewulf and Langenhove, 1997). On the other hand similar retention times for different isomers of one species and complications due to chemical loss in the sampling procedure, e.g. of cresol isomers may cause problems. In contrast to that, spectroscopic techniques allow a direct in-situ detec-

tion without wall losses. Aromatic hydrocarbons absorb radiation in both, the infrared (IR) and ultraviolet (UV) spectral range, and until now, were detected by Fourier Transform InfraRed (FTIR) (Fateley *et al.*, 1995) spectroscopy (2.5–14 μm) as well as by Differential Absorption Light Direction and Ranging (Differential Absorption LIDAR or DIAL) (Milton *et al.*, 1992) and Differential Optical Absorption Spectroscopy (DOAS) in the UV region (240–290 nm) (Axelsson *et al.*, 1995; Trost, 1997). UV spectroscopic techniques prove to be more sensitive than FTIR. DOAS detection limits for a number of aromatic VOCs are well below one ppb, while DIAL detection limits for benzene and toluene, the only compounds detected with DIAL so far, are of the order of a few ppb.

1.4. DOAS measurements of aromatic hydrocarbons

DOAS is based on detecting narrow absorption features of molecules, which absorb light following Lambert–Beer's law:

$$D = \ln \frac{I_0(\lambda, L)}{I(\lambda, L)} = \left[\sum_{i=1}^n \sigma_i(\lambda) C_i + \mu_{\text{Rayleigh}}(\lambda) + \mu_{\text{Mie}}(\lambda) \right] L. \quad (1)$$

Equation (1) defines the optical density D , where $I_0(\lambda, L)$ represents the light intensity in the absence of any extinction and $I(\lambda, L)$ is the remaining intensity after the light has been reduced by attenuation due to Rayleigh- and Mie-scattering (absorption coefficients $\mu_{\text{Rayleigh}}(\lambda)$ and $\mu_{\text{Mie}}(\lambda)$) as well as by several atmospheric absorbers (n absorbers, absorption cross section $\sigma_i(\lambda)$, concentration C_i) (Platt and Perner, 1983). The quantity L represents the absorption path length in the atmosphere (typically a few 100 m to some 1000 m).

High-pass filters remove broadband (continuum) variation of the cross section as well as the wavelength dependency of the measured spectra due to Rayleigh- and Mie-scattering and the lamp. Reference spectra ($\sigma(\lambda)$) taken in the laboratory then allow each absorber to be identified by its specific "fingerprint" in the measured spectrum using nonlinear least square fitting (Stutz and Platt, 1996). Concentrations of the respective species are then calculated from the fit coefficients using Lambert–Beer's law. If all absorbers that show absorption in the observed wavelength interval are removed from the measured spectrum by subtracting their scaled reference spectra, a residual structure will remain, basically representing the electronic noise of the instrument. Major advantages of the DOAS technique are the absence of wall losses e.g. in sampling tubes, a good time resolution (see Table 1) and its inherent calibration, which only depends on the cross sections applied for data evaluation (Platt, 1994).

DOAS measurements of monocyclic aromatic hydrocarbons in the atmosphere so far include benzene, toluene (Loefgren, 1992; Sandroni *et al.*, 1994;

Table 1. Measurement techniques for aromatic hydrocarbons in the atmosphere. The major advantage of gas chromatographic measurement techniques are low detection limits, meanwhile spectroscopic measurement techniques allow a non-invasive and inherently calibrated detection of e.g. aromatic hydrocarbons. With these techniques DOAS proves to be most sensitive

Measurement Technique	Detectable aromatic hydrocarbons	Time resolution	Sensitivity	References
GC-FID	Benzene Toluene Xylene-Isomers ⋮	20 min to 1 h 30 min	0.3–1.2 ppt	Nutmagul and Cronn (1985) Greenberg <i>et al.</i> (1994)
GC-MS	Benzene Toluene Xylene-Isomers ⋮		0.5–1.8 ppt	Helmig and Greenberg (1994) Dewulf <i>et al.</i> (1996)
GC-PID	Benzene Toluene Xylene-Isomers ⋮		0.5–2 ppt	Rudolf <i>et al.</i> (1986)
REMPI-TOF MS	Benzene Toluene Xylene-Isomers	10 ms	1 ppm 1 ppm 1 ppm	Franzen <i>et al.</i> (1995)
FTIR	Benzene Toluene Xylene-Isomers ⋮		4 ppb ^a 6 ppb ^a 2 ppb ^a	Fateley <i>et al.</i> (1995)
DIAL	Benzene Toluene	25 s to 20 min	10 ppb 5 ppb	Milton <i>et al.</i> (1992) Weitkamp <i>et al.</i> (1996)
DOAS	Benzene Toluene <i>p</i> -Xylene <i>m</i> -Xylene <i>o</i> -Xylene Benzaldehyde Ethylbenzene Styrene Trimethylbenzene-Isomers Phenol <i>p</i> -Cresol <i>m</i> -Cresol <i>o</i> -Cresol Dimethylphenol-Isomers	1 min ^b to 30 min ^c	0.2 ppb ^b –0.8 ppb ^c 0.2 ppb ^b –0.7 ppb ^c 0.1 ppb ^b –0.4 ppb ^c 0.4 ppb ^b –1.5 ppb ^c 0.8 ppb ^b –3.4 ppb ^a 46 ppt ^b –190 ppt ^a 560 ppt ^b –2.4 ppb ^a 122 ppt ^b –510 ppt ^a 0.6 ppb ^b –2.6 ppb ^a 14 ppt ^b –60 ppt ^c 19 ppt ^b –80 ppt ^a 65 ppt ^b –270 ppt ^a 86 ppt ^b –360 ppt ^a < 0.7 ppb ^b –< 3 ppb ^a	This work

^a Corresponding pathlength $L = 480$ m.

^b Long path DOAS, path length $L = 2000$ m, 0.15 nm resolution, calculated from Etzkorn *et al.* (1998).

^c White Cell DOAS, path length $L = 480$ m, 0.15 nm resolution, observed in this work.

Partridge *et al.*, 1995; Ottobriani *et al.*, 1996), xylene-isomers (Conner and Stevens, 1991; Wilkerson *et al.*, 1992; Barrefors, 1996), benzaldehyde (Pitts *et al.*, 1984; Trost, 1997), ethylbenzene, trimethylbenzene-isomers (Axelsson *et al.*, 1995; Brocco *et al.*, 1997) and phenol (Trost, 1997). DOAS measurements of cresol-isomers are reported from outdoor smog chamber experiments (Etzkorn, 1998; Martín-Reviejo *et al.*, 1996).

1.5. Problems with DOAS measurements of aromatic species in the atmosphere

The major problem with DOAS measurements of aromatic hydrocarbons is oxygen interference with the aromatic species, as illustrated in Fig. 1 for some of the most important aromatic species in the atmosphere. Overlap of oxygen absorption consequently has to be accounted for, when reliable measurements

of aromatic concentrations in semipolluted urban air and rural air are to be carried out. In the DOAS literature on measurements of aromatic hydrocarbons only sparse information is given about the correction of the O₂ absorption (Wilkerson *et al.*, 1992; Brocco *et al.*, 1997). Conner and Stevens (1991) simultaneously measured benzene concentrations by GC techniques and DOAS on two different light paths with different path lengths. They found average concentrations of benzene (averaged over a period of several weeks) measured by DOAS to be 60% higher on the short light path and to be 120% higher on the long light path than the corresponding 'GC' concentrations, which in part might be due to O₂ contribution to the benzene signal at low resolution. Sandroni *et al.* (1994) state that benzene data need an offset adjustment. Moreover, Wilkerson *et al.* (1992) found

striking discrepancies with DOAS measurements of toluene and suggests O₂ interference as a possible error source.

For atmospheric conditions no reference spectrum of the Herzberg bands is available in the literature, and the O₂ absorption, if accounted for at all, was corrected by a “zero” reference spectrum taken in “clean” air (Axelsson *et al.*, 1995; Trost, 1997). The disadvantage of this method is that it only allows access to the variations of the aromatic concentrations in the atmosphere, and introduces an unknown negative offset for all species present in the “zero” spectrum, as this spectrum is subtracted from each measured spectrum.

To characterize the magnitude of the O₂ interference with DOAS measurements of aromatic hydrocarbons the signal of benzene in a measured spectrum can be compared to that of the nearby O₂ band at 259 nm. At a path length of 500 m, atmospheric O₂ bands have an optical density (see equation (1)) of $\approx 8 \times 10^{-2}$ (measured value) at a resolution of 0.15 nm. Assuming a mixing ratio for benzene of 2 ppb, a typical level in the urban air of Heidelberg, the optical density of the benzene absorption will be 2.5×10^{-3} . That means, that the O₂ absorption will dominate the measured spectrum being larger by a factor of ≈ 30 than the benzene signal. Fortunately, most aromatic species show their strongest absorption bands towards longer wavelength, where the O₂ absorption is weaker (see Fig. 1), but still the O₂ absorption bands are likely to be stronger than the aromatic absorption, since most aromatics are present at lower concentrations than benzene.

In fact, DOAS measurements of aromatic hydrocarbons pose further problems that are not necessarily related to the O₂ interference. Comparison of atmospheric DOAS long path measurements of aromatic hydrocarbons (benzene, toluene, *o*-, *p*-xylene) with simultaneous measurements using GC techniques at several points along the light pass have demonstrated correlations of varying quality (Conner and Stevens, 1991; Lofgren, 1992; Barrefors, 1996) suggesting that interference effects (see below) and incorrect calibration may explain the differing results. Good correlations were found only in homogeneously mixed rural air with poorer correlations at low concentrations (Lofgren, 1992) where O₂ interference is a major problem.

Barrefors (1996) found poor correlation of long-path DOAS data with simultaneously measured GC data, that can not be explained by inhomogeneities of the atmosphere. He suggests, that severe interference effects due to the simultaneous presence of several aromatic hydrocarbons with similar spectra may be the cause for incorrect DOAS results. Similar considerations were first mentioned by Conner and Stevens (1991) and are discussed in more detail by Axelsson *et al.* (1995). Partly these problems are due to low resolution of the spectrometers used for the measurements. The overlap of spectral structures of indi-

vidual aromatic species (see Fig. 1) in principle is no problem for DOAS measurements (with the exception of higher alkylbenzenes), since at the resolution of the cross sections shown the absorption bands are well separated. Furthermore, the high pass filters applied in the evaluation procedure can be optimized to reduce cross sensitivities (see Section 3.3.1). Another, more general problem is due to the calibration of the measurements. In the literature only sparse information is given on the absorption cross sections used for the calibration of DOAS measurements of aromatic hydrocarbons (see Etzkorn *et al.*, 1998 for details).

1.6. The Herzberg bands of O₂

In the UV spectral region below 300 nm O₂ molecules show weak absorption due to electronic excitation in the Herzberg I ($A^3\Sigma_u^+ \leftarrow X^3\Sigma_g^-$), Herzberg II ($c^1\Sigma_u^- \leftarrow X^3\Sigma_g^-$) and Herzberg III ($A'^3\Delta_u \leftarrow X^3\Sigma_g^-$) transitions, the latter giving rise to additional diffuse absorption bands due to O₂-dimers. Classified as electric dipole forbidden transitions, the Herzberg bands gain strength by inner mixing processes (Kerr and Watson, 1986; England *et al.*, 1996). All four band systems strongly overlap, extending from the joint dissociation limit of O₂ at 242.9 nm towards longer wavelengths with the absorption becoming negligible above 287 nm.

Since their discovery by Dr. Gerhard Herzberg (Herzberg, 1932, 1952) the Herzberg bands have been extensively studied in the past to quantitatively understand odd oxygen (O, O₃) formation (Chapman cycle) in the stratosphere, most recently in conjunction with the “ozone deficit problem” (Miller *et al.*, 1994). Measurements on the Herzberg band systems were therefore carried out in order to quantify the relative contributions of the three transitions to the absorption in the Herzberg continuum, which at wavelengths shorter than 242.9 nm adjoins the Herzberg bands and is a primary source for ³P oxygen atoms in the stratosphere (Amoruso *et al.*, 1996). Theoretical approaches were made to estimate potential curves of the Herzberg states and transition moments of the Herzberg band systems. More accurate molecular constants of the $X^3\Sigma_g^-$ ground state and the $A^3\Sigma_u^+$, $c^1\Sigma_u^-$, $A'^3\Delta_u$ Herzberg states were determined by Ramsay (1986), Borrell *et al.* (1986) and Coquart and Ramsay (1986), who re-examined Herzberg’s work using longer absorption paths and higher resolution. Huestis *et al.* (1994) used the discrete structure of the Herzberg bands below 258 nm to calculate absolute oscillator strengths for all three systems, showing the Herzberg I transition to be more than one order of magnitude stronger than the Herzberg II and Herzberg III systems. Recently, Yoshino *et al.* (1994) presented rotationally resolved data of the Herzberg I bands below 270 nm yielding significantly higher results for the absolute oscillator strength than Huestis *et al.* (1994), which is in agreement with data from other authors (Hasson and Nicholls, 1971; Bao *et al.*, 1995). England *et al.* (1996) used Yoshino’s data

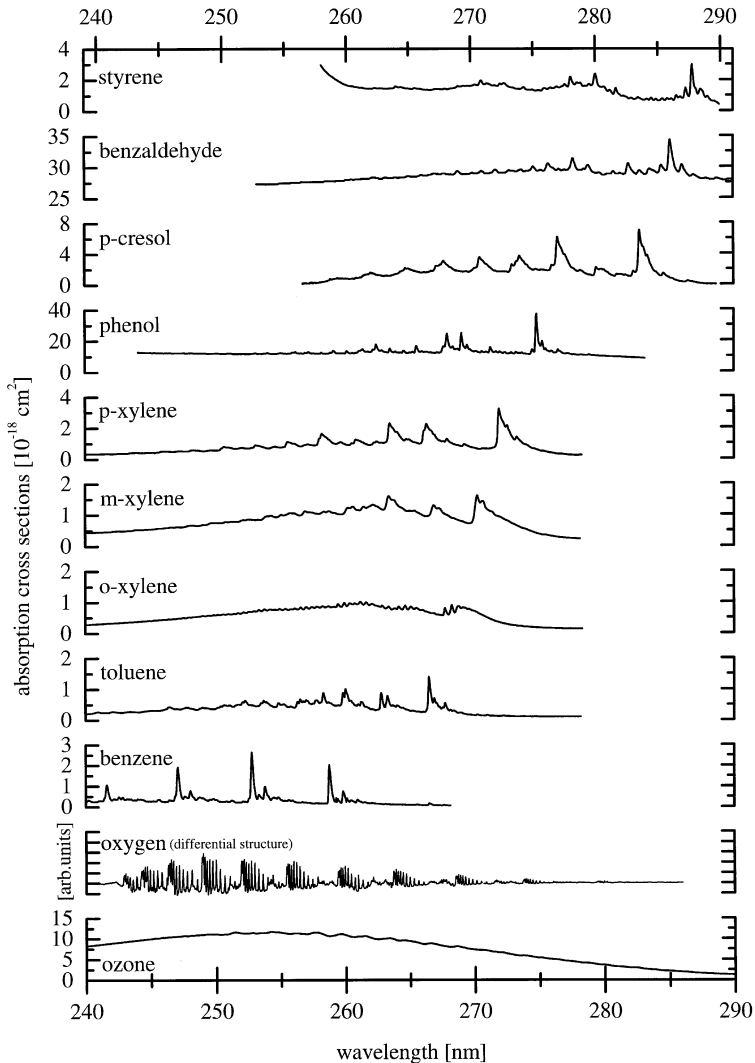


Fig. 1. Interference of O_2 with the DOAS measurement of aromatic species: Comparison of the differential structure of O_2 (Herzberg band system) as described in Section 2.1 with the absorption cross sections of some of the most important aromatic hydrocarbons in the atmosphere (Trost *et al.*, 1997). The strong spectral overlap of oxygen absorption with aromatic absorption bands is clearly visible. In most cases, oxygen absorption in a measured spectrum will be stronger by an order of magnitude than the aromatic absorption features.

to calculate absolute electronic transition moments for the Herzberg I bands obtaining quantitative agreement with the experiment with respect to absolute band oscillator strength.

Regarding the transparency of the ground level atmosphere in the UV (below 300 nm), Ditchburn and Young (1962) concluded that attenuation by O_2 in the Herzberg systems is comparable to extinction by tropospheric ozone and consequently has to be taken into account in transparency calculations (Trankovsky *et al.*, 1989). Nevertheless these calculations do not include attenuation by the dimer, which might be comparable with O_2 and ozone at wavelengths below 260 nm (Dianov-Klokov, 1966a). Table 2 summarizes the properties of the individual Herzberg band systems, the spectroscopic notation of these transitions

and the respective violated selection rules. The oscillator strength f given in Table 2 only refers to the structured absorption of the Herzberg bands neglecting contribution of the Herzberg continuum. In the case of the Herzberg I transitions of O_2 , both contributing electronic states $A^3\Sigma_u^+$ and $X^3\Sigma_g^-$ show a triplet splitting of rotational levels. This fine structure causes each observed Q-branch to consist of seven individual Voigt-shaped ro-vibronic lines and the weaker O- and S-branches to consist of three lines, respectively (Herzberg, 1952).

1.7. The O_2 -dimer absorption

Additionally broad band absorptions (full width at half maximum ≈ 3 nm) superimpose the molecular discrete structure of the Herzberg bands as a system of

Table 2. Spectroscopic properties of the Herzberg transitions. The transition probability of these forbidden band systems is reduced by a factor of about 10^{-7} as compared to allowed electronic transitions. Comparing the oscillator strength f it is seen that the Herzberg I band system dominates the oxygen absorption in the Herzberg bands between 243 and 287 nm. Due to the fine structure of the participating triplet states, this band system appears as a series of Q -branches, with each Q -branch consisting of seven lines (see text)

System	Spectroscopic notation	Selection rule violated ^a	Oscillator strength f	Relative strength
Herzberg I	$A^3\Sigma_u^+ \leftarrow X^3\Sigma_g^-$	$\Sigma^+ \leftrightarrow \Sigma^-$	8.64×10^{-10b}	22
Herzberg II	$c^1\Sigma_u^- \leftarrow X^3\Sigma_g^-$	$\Delta\Sigma \neq 0$	$\approx 4 \times 10^{-11c}$	1
Herzberg III	$A'^3\Delta_u \leftarrow X^3\Sigma_g^-$	$\Delta\Lambda = 0, \pm 1$	$\approx 10^{-10c}$	2.5

^a Herzberg (1952).

^b Calculated from Yoshino *et al.* (1995) using relative strength for (3–0) to (0–0) transitions from recommended strengths by Huestis *et al.* (1994).

^c Calculated from relative strength to Herzberg I given by Huestis *et al.* (1994).

diffuse triplets. Warburg (1915) first mentioned a quadratic pressure dependence of the absorption of gaseous oxygen at these wavelengths and Wulf (1928) first ascribed this behavior to the formation of oxygen dimers (O_4). With regard to the dimer's nature Van der Waals molecules in (1) bound, (2) metastable form and (3) colliding pairs are discussed. Only bound Van der Waals dimers should exhibit structured absorption features, possibilities (2) and (3) would result in broadened absorptions. In any case, dimer formation forces the cross section to increase linearly with pressure, which for dimer absorption in the Herzberg band's wavelength range was observed in pure oxygen gas (Finkelnburg and Steiner, 1932; Shardanand, 1969) as well as in mixtures with other gases, e.g. nitrogen, argon (Warburg, 1915; Dianov-Klovov, 1966a; Shardanand, 1977; Johnston *et al.*, 1984). Dianov-Klovov (1966a) found the observed diffuse triplets in O_2/N_2 mixtures under pressures up to 20 bar and at a temperature of $T = 293$ K, to be analogous to the Herzberg III transition. These were classified as absorption of O_2-O_2 and O_2-N_2 collision complexes in the Herzberg III system of oxygen with the transition probability in the complexes increased by two (Blake and McCoy, 1987) to three (Dianov-Klovov, 1966a; Johnston *et al.*, 1984) orders of magnitude as compared to the unperturbed molecular transition. Moreover, he found the O_2-N_2 complex to be a half as strong absorber as the O_2-O_2 complex, leading to a predominant fraction (66%) of the dimer absorption to be due to O_2-N_2 complexes under atmospheric conditions. Dimer absorption begins to dominate O_2 absorption at a pressure of about 4 bar of pure O_2 (Dianov-Klovov, 1966a).

With regard to the nature of the dimer, temperature dependence studies on dimer absorption find diverse results for the enthalpy of formation (ΔH_f) of bond type Van der Waals dimers ranging from $\Delta H_f = -1.1 \pm 0.5$ kcal/mol⁻¹ (Orlando *et al.*, 1991) to be essentially zero ($\Delta H_f = -0.2 \pm 0.4$ kcal/mol⁻¹) (Horowitz *et al.*, 1989). Nevertheless recent progress in modelling Van der Waals molecules' potential surfa-

ces (Epifanov and Vigin, 1994) strongly support the classification of oxygen dimers under atmospheric conditions as mixtures of metastable Van der Waals dimers and colliding pairs (Perner and Platt, 1980; Dianov-Klovov, 1966b; Horowitz *et al.*, 1989; Greenblatt *et al.*, 1990).

1.8. Problems in measuring oxygen reference spectra in the laboratory

The measurement of oxygen reference spectra poses several problems:

1. Due to the low transition probability of the forbidden Herzberg bands, long light paths (a few hundred meters to a few kilometers) comparable to those used in the atmospheric detection of aromatic hydrocarbons are needed, which in the laboratory only can be reached by the use of a multireflexion cell, e.g. a White system (White, 1976).
2. The Herzberg bands consist of a series of narrow ro-vibronic lines with a width of the order of 1 pm. In order to fully resolve these lines a spectral resolution well below 1 pm would be required. If at a lower resolving power the individual lines can not be separated the apparent optical density will not increase linearly with the O_2 concentration. As a consequence, the shape of the spectral features will depend on the O_2 column density and i.e. for each observed O_2 column density an individual O_2 reference spectrum is needed (see Section 3.1). In the laboratory this can be accounted for by varying the observed O_2 column density by changing the O_2 partial pressure.
3. When the O_2 partial pressure is changed, additional problems arise due to absorption of O_2-O_2 and O_2-N_2 dimers that overlap the discrete O_2 lines of the Herzberg bands as relatively broad band absorptions (see Section 1.7). While absorption features of O_2-O_2 and O_2-N_2 are also present in the atmospheric spectra, their relative strength scales differently than the O_2 partial pressure and

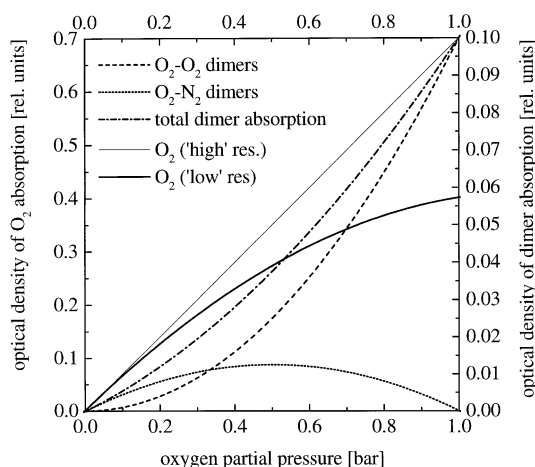


Fig. 2. Calculated optical densities of O₂ at “high” and “low” spectral resolutions as well as dimer absorption to illustrate the problem of the oxygen correction. At “low” resolution, the apparent optical density of O₂ yields saturation as the O₂ partial pressure is increased. Dimer absorption is shown for O₂-O₂ dimers and O₂-N₂ dimers separately. Due to the presence of N₂, the measured dimer absorption (equal to the sum) varies less than quadratic with the O₂ partial pressure (see text).

needs to be separated in order to use the oxygen references measured at different O₂ partial pressures (see Section 2.2).

- To enhance the quality of the measurements of atmospheric trace gases, DOAS spectra taken with a White system can be evaluated as quotient spectra of a long (720 m) and a short (240 m) path length to give an effective absorption path of 480 m (see Section 2.2). In the case of O₂ absorption in the Herzberg bands the above mentioned nonlinear effects cause this quotient spectra not to reflect the relative strength of the absorption bands as they would be observed at a path length of 480 m in the atmosphere.

Figure 2 illustrates the above mentioned problems and roughly scales the molecular and dimer absorption as observed under our experimental conditions. The saturation effect of the apparent molecular absorption with increasing O₂ concentration can be seen at “low” resolution (fat line in Fig. 2) if compared to that at “high” resolution (straight line in Fig. 2, scaled to fit into the diagram). The O₂-O₂ dimer absorption should increase quadratically with the O₂ partial pressure (dashed line in Fig. 2). The O₂-N₂ dimer absorption peaks at O₂ and N₂ being present at equal concentration (dotted line in Fig. 2). Even though the presence of N₂ reduces the quadratic increase of total dimer absorption (dashed dotted fat line in Fig. 2), total dimer absorption varies nonlinearly with the O₂ partial pressure.

We here present oxygen reference spectra, which allow to virtually eliminate the O₂ interference in

atmospheric measurements of aromatic hydrocarbons.

2. EXPERIMENTAL

2.1. Recording of the oxygen reference spectra

Measurements were performed using a White type *f*/100 multireflection cell (White, 1976) improved for stability (Ritz *et al.*, 1992) with a basepath of 15 m. The mirrors were coated with aluminium and spectra were taken at 16 and 48 traverses, corresponding to 240 and 720 m absorption paths, respectively.

The system was mounted inside a reference cell (see Fig. 3) consisting of two aluminium cases for mirror protection (equipped with gas inlet ports, water manometers and a quartz window for light beam in- and output), which were connected by a hose made of teflon sheet (120 μm thickness, 450 mm diameter) flange mounted to both cases. The reference cell was flushed and filled with oxygen (99.995% purity ≡ grade 4.5) and mixtures of O₂/N₂ (grades 4.5/5.0) at pressures slightly exceeding atmospheric pressure ($\Delta p < 1$ mbar). Gases were premixed by the manufacturer and taken from gas tanks connected by teflon tubes to the gas inlet ports of the cell. Leakage of the system was compensated by a massflow controlled gas inlet during the experimental runs.

The transfer optics used to match the *f*-numbers of the White system and the spectrograph consisted of two separate Newton telescopes. A quartz fibre mode mixer (Stutz and Platt, 1997) was inserted between the transfer optics and the spectrograph in order to provide for homogeneous illumination of the spectrograph/detector system. A *f*/6.9 Czerny Turner spectrometer (ACTON 500) with two reflection gratings interchangeable under computer control (3600 grooves mm⁻¹, 68 × 68 mm², blaze: 240 nm; 1200 grooves mm⁻¹, 68 × 86 mm², blaze: 300 nm) was used, which was thermostated to $T = 30 \pm 0.1^\circ\text{C}$. The spectrograph slit width was set to 80 μm yielding a spectral resolution (FWHM of an atomic emission line) of 0.05, 0.15 nm (0.16 nm for atmospheric measurements) for the two gratings, respectively. A photodiode array detector (Stutz and Platt, 1992) (Reticon, 1024SRU-011, 1024 diodes of 25 μm center to center spacing, height: 2.5 mm) flange mounted to the spectrograph was used for detecting the spectra. The array was cooled by a three stage peltier cascade with a forced air cooled heat sink to $T = -40^\circ\text{C}$ in order to reduce dark current to less than 6% (3600 grooves mm⁻¹ grating) and 0.5% (1200 grooves mm⁻¹ grating) of the

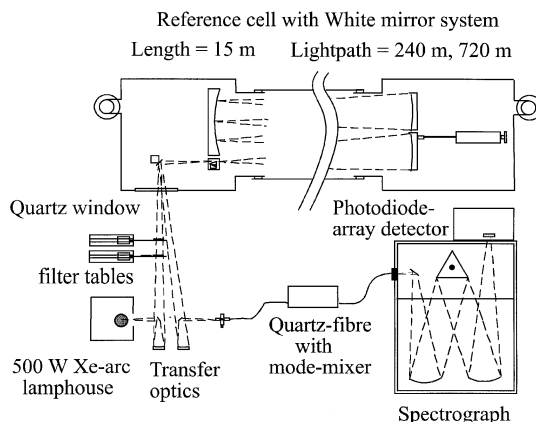


Fig. 3. The experimental setup. See text for details.

Table 3. Column densities of the oxygen/nitrogen mixtures investigated. Relative enhancement factors of the dimer absorption were calculated by dividing the nonlinearly increasing dimer absorption by the factor O_2 is scaled relative to 21% O_2 . In pure oxygen, dimer absorption will be 8 times higher than under atmospheric conditions, which must be divided by the roughly five times higher O_2 concentration to give the relative enhancement factor of 1.65

O_2/N_2 conc. ratio (%)	Temperature T (K)	Column density ^a $C \cdot L$ (10^{23} molecules cm^{-2})	Equivalent ^a path length (m)	Relative enhancement of the dimer absorption ($D(\text{Dimer})/D(\text{Dimer}_{\text{atm}})/[O_2]/[O_2]_{\text{atm}}$)
10	294.5	0.60 (1.79)	114 (341)	0.91
20.6	294	1.22 (3.66)	232 (697)	0.98
40	294	2.37 (7.11)	451 (1354)	1.16
60.1	295	3.58 (10.73)	682 (2046)	1.32
80.2	293	4.76 (14.27)	907 (2720)	1.49
99.995	295.5	5.95 (17.85)	1133 (3400)	1.65

^a For short path length, data for long path length are given in brackets.

Table 4. Observed spectral intervals. Two sets of oxygen reference spectra were recorded at different resolution. At wavelengths below 300 nm, the relative fraction of stray light increases as the light intensity emitted by the lamp decreases. Especially with measurements at high resolution (0.05 nm FWHM) stray light needs to be removed from the measured spectra (see text)

Observed wavelength intervals (nm–nm)	Estimated error due to straylight after correction (%)	Resolution (nm)	Resolving power R
3600 grooves mm^{-1} grating			
240–250	< 6	0.051	4800
250–260	< 4	0.051	5000
260–270	< 3	0.050	5300
269–279	< 3	0.051	5375
279–289	< 2	0.051	5570
1200 grooves mm^{-1} grating			
225–265	< 1	0.15	1630
250–290	< 0.1	0.15	1800

signal, respectively. The software system MFC 1.98 (Gomer *et al.*, 1993) provided for automatic data acquisition as well as control of the spectrometer and the stepper motors that were used to change the light path of the White system and to place the filter for the stray light measurements.

For the measurements the spectrograph was operated in the spectral range between 240 and 290 nm. Different spectral intervals were observed as summarized in Table 4. For each gas filling spectra were taken at 240 m (short) and 720 m (long) absorption path. Oxygen/nitrogen concentration ratios investigated are given in Table 3, together with the equivalent path length under atmospheric conditions (21% oxygen) and the temperature of the gas filling. The relative enhancement of dimer absorption with increased O_2/N_2 concentration ratios is also given in Table 3 divided by the factor that the O_2 concentration is enhanced as compared to 21% mixing ratio. Integration times were adjusted to reach at least 60% (25% in the deeper UV at high resolution) of the detector saturation and typically were 25–100 s for the 1200 grooves mm^{-1} grating, not exceeding 400 s for the 3600 grooves mm^{-1} grating. Spectrometer stray light was reduced by placing a UG5 bandpass filter (Schott) of 3 mm thickness in the lightbeam. Spectra were coadded in sets of ten and stored to disk. Additionally, with each measured spectrum, a stray light spectrum was taken. This was done by placing a cut off filter in the light path, blocking the light below 300 nm but transmitting most of the light from other wavelengths. All measured spectra were corrected for (1) stray light, (2) dark current and (3) electronic offset. Straylight and dark current were corrected for by subtracting the stray light spectrum from the measured spec-

trum. The estimated error is given for each observed spectral range in Table 4. Electronic offset was measured separately in the laboratory and subtracted from the measured spectrum. In a next step the 720 m spectrum was divided by the 240 m spectrum to eliminate detector etalon structure, lamp structure and effects of variations in the sensitivity of individual photodiodes. About six ratio spectra (consisting of ten coadded individual spectra) of one wavelength interval were adjusted for thermal shifts and then added to further minimize total noise. Spectral shift was found to be less than 4×10^{-3} (corresponding to 2.5 μm on the diode array) due to the thermostated spectrometer.

As an example, Fig. 4 shows a spectrum taken in pure oxygen with an absorption path length of 240 m at 0.05 nm spectral resolution.

2.2. Atmospheric measurements

Measurements were carried out 20 m above the ground using a very similar experimental setup as the one described above, with the teflon hose removed, and the equipment mounted on the flat roof of the institute building. Lamp, transfer optics, spectrometer/detector system and control units were placed inside a temperature stabilized measurement container. The White-system itself was set up outside the container with a window in the container wall allowing light input and output.

Spectra were recorded in the wavelength interval from 250 to 290 nm at a slightly lower spectral resolution (0.16 nm) than in the laboratory using the 1200 grooves mm^{-1} grating.

Prior to the atmospheric measurements, reference spectra of benzene, toluene, *p*-xylene, *m*-xylene and phenol were

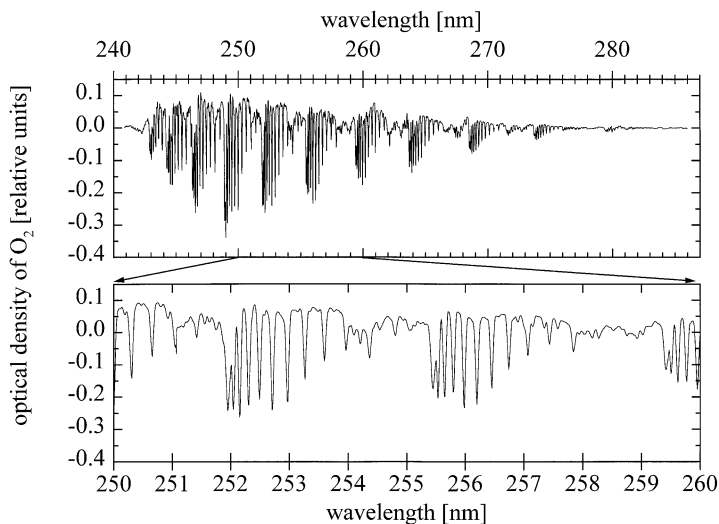


Fig. 4. Oxygen reference spectrum of the Herzberg bands taken in pure O_2 at a resolution of 0.05 nm. The spectrum was taken with 240 m absorption path length and corrections were applied as described in the text. Shown is the logarithm of the spectrum which was high pass filtered using a 5000 times triangular smoothing routine. The strong Q -branches of the Herzberg I band dominate the spectrum (see text).

recorded in the same experimental setup by sequentially placing a gas cell sample of each compound in the light beam. Spectra were taken on the short light path with and without the gas cell sample inserted in the light path. With each spectrum a stray light spectrum (see Section 2.1) was recorded and spectra were corrected as described above. By dividing the spectrum with the sample by the spectrum without the sample inserted in the light path, detector etalon, lamp structure, diode effects and absorption due to atmospheric absorbers were eliminated. The thus obtained gas cell reference spectra were calibrated using the absolute cross sections remarked by Etzkorn *et al.* (1998). For the evaluation of atmospheric spectra, interfering absorption features of oxygen, ozone and sulfur dioxide were taken into account. Two oxygen reference spectra (ratio spectra taken in 21% and 40% O_2) were used to account for the nonlinearities caused by atmospheric density variations, as described in Section 3.1. Ozone absorption cross sections depend on temperature. A variation of ambient temperature of some ten degrees, therefore, introduces residual structures if only a single ozone reference spectrum for a particular temperature is fitted to the measured spectra. Ozone reference spectra were taken from Bass and Paur (1985) for three temperatures ($T = 273, 278, 295$ K) and adjusted to the resolution of the spectrometer to account for this temperature dependence. The SO_2 reference spectrum was measured as described for the aromatic species and absolute cross sections were taken from (Vandaele *et al.*, 1994) for calibration.

Atmospheric spectra were recorded at short (240 m) and long (720 m) light path and corrections were performed as described above. The resulting effective absorption path length was 480 m. Time resolution of the measurements varied between 20 and 45 min, depending on the visibility in the atmosphere.

All divided atmospheric spectra (see Section 2.1) and all reference spectra (except the oxygen reference spectra) were subsequently convoluted with the instrument function of the oxygen reference spectra. In the same way, the oxygen references were convoluted with the instrument function of the atmospheric setup. In this way, congruent spectral features were established in the reference- and the measured spectra. In the next step, the spectra were high pass filtered. While frequently polynomial- or triangular filtering algorithms were used (the spectrum is divided by a fitted polynomial of

suitable degree or by a smoothed copy of itself) (Axelsson *et al.*, 1995; Barrefors, 1996; Brocco *et al.*, 1997) we preferred a filter based on Savitzky Golay smoothing (Savitzky and Golay, 1964). This flexible smoothing routine allows on the one hand, to almost eliminate the absorption due to dimers and on the other hand, to optimize a high pass filter with respect to the detection limit of individual species. The latter was done by evaluating the atmospheric spectra for different high pass filters to obtain the respective size of the mean residual structure after subtraction of all reference spectra. If the differential optical density of each high pass filtered reference spectrum is compared to the respective residual in the wavelength interval of interest, the thus defined signal to noise ratio can be maximized for each species. The high pass filtered reference spectra were adjusted to the measured spectra using nonlinear least squares fitting routines (Stutz and Platt, 1996) in the wavelength interval from 257 to 283 nm. Eleven reference spectra, i.e. two oxygen reference spectra (21% O_2 , 40% O_2 , i.e. bracketing the atmospheric O_2 column density), three ozone reference spectra (273 K O_3 , 278 K O_3 , 295 K O_3), SO_2 , benzene, toluene, *p*-xylene, *m*-xylene and phenol reference spectra were used. Since the number of reference spectra, that can be fit simultaneously by our software (Gomer *et al.*, 1993) was limited to nine, evaluation had to be done in two sequences. In a first step, benzene, toluene, *p*-xylene, *m*-xylene and phenol reference spectra were fit together with the two oxygen reference spectra, the 278 K O_3 and SO_2 reference spectra. In a second step, the 273 K O_3 and 295 K O_3 reference spectra were adjusted to the residual of the first fit procedure. Hence, all aromatic species were fitted simultaneously in the first step. No spectral shift was allowed for aromatic reference spectra. The oxygen reference spectra were shifted to coincide in their relative band positions, fixed in this position and were allowed only simultaneous shifts when fitted to the atmospheric spectra. In the same way, the ozone reference spectra of the second fit procedure were allowed only simultaneous shifts.

Figure 5 shows examples of the evaluation of an atmospheric spectrum. Sequentially, all reference spectra are subtracted from the atmospheric spectrum (top thin line), the thick line is a reference spectrum composed of both oxygen reference spectra, all three ozone reference spectra and SO_2 as scaled by the fit. The remaining residual structure after

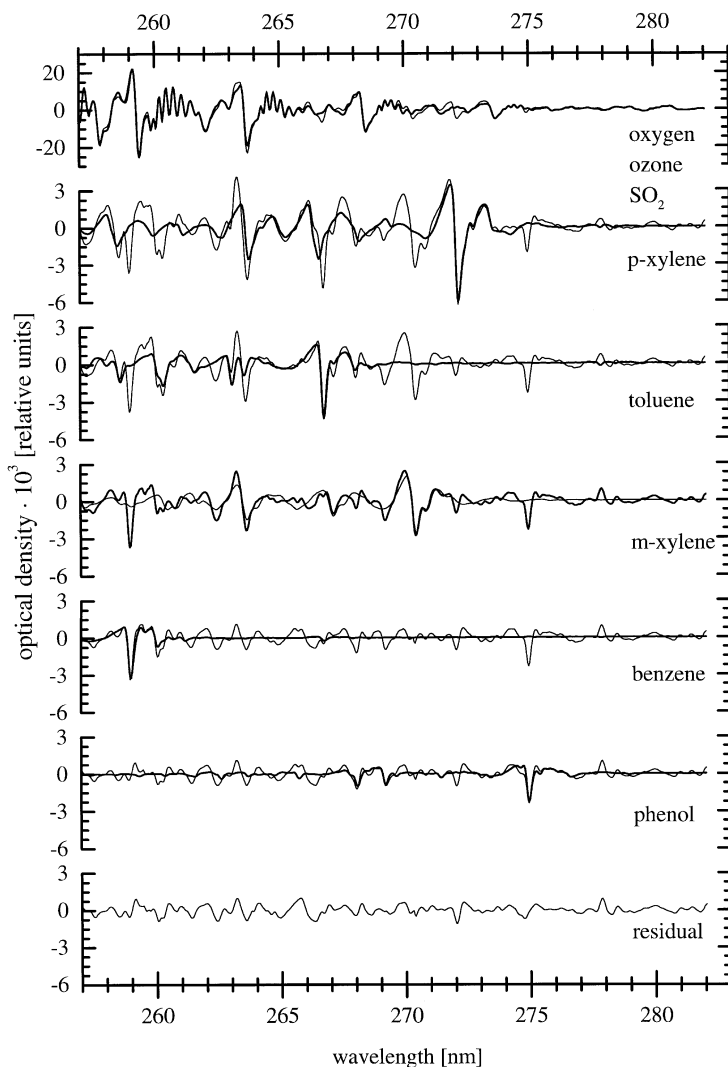


Fig. 5. Example for the evaluation of atmospheric DOAS measurements of aromatic hydrocarbons. The atmospheric DOAS spectrum, taken on 7 February 1997, 18:30 local time is shown as the thin line on the top. The thick line is a reference spectrum composed of oxygen, ozone and SO₂ reference spectra. The remaining residual after subtracting this reference spectrum is shown below, clearly showing absorption bands of *p*-xylene (thick line). In the next line *p*-xylene is subtracted and a toluene reference spectrum (thick line) is overlaid on the remaining residual structure (thin line). In this way, *m*-xylene, benzene and phenol reference spectra are subtracted. The remaining residual structure is shown at the bottom. Mean residual structures over the period of observation were found to be 1.3×10^{-3} (peak to peak).

subtracting these reference spectra is shown below with the reference spectrum of *p*-xylene showing strongest absorption bands in the residual structure being overlaid, and subtracted in the next line. Subsequently, the reference spectra are overlaid and subtracted from the respective residual structure in the sequence determined by the strength of the respective absorptions. At the bottom of Fig. 5 the residual structure after subtraction of all reference spectra is shown.

Concentrations of aromatic species, ozone and SO₂ were then calculated from the fit coefficients of the calibrated reference spectra. Only the aromatic concentrations will be presented here. Over the period of observation the mean size of the residual structure was 1.3×10^{-3} (peak to peak). Mean detection limits were calculated for each detected species from the mean residual and the "differential" cross section that remains after the broad band variation is removed by the high-pass filter and are given in Table 5.

The total error of the measured mixing ratios is due to the experimental error of the DOAS system ($\approx 5\%$, due to e.g. noise and stray light (Volkamer, 1996)), the error of the evaluation procedure ($<10\%$) and the error of the cross sections used for the calibration ($<5\%$). Accordingly, the measured mixing ratios are estimated to be accurate within an error of 12%.

3. RESULTS AND DISCUSSION

3.1. Model calculations on the elimination of the Herzberg bands

Model calculations on the 5-0 band of the Herzberg I band system were carried out for two reasons:

Table 5. Measured concentrations of aromatic species. Absorption features of benzene, toluene, *p*-xylene and phenol were detected in almost each measured spectrum, meanwhile that of *m*-xylene were detected only occasionally due to the smaller cross section of this compound. This is reflected by the observed mean concentrations as they are compared to the mean detection limit during the period of observation

Species	Maximum mixing ratio (ppb)	Mean mixing ratio (ppb)	Mean absolute error (ppb)	Mean detection limit (ppb)
Benzene	3.8	1.8	± 0.2	0.8
Toluene	7.6	2.5	± 0.2	0.7
<i>p</i> -Xylene	4.8	0.8	± 0.1	0.4
<i>m</i> -Xylene	10.2	1.2	± 0.2	1.4
Phenol	0.24	0.077	± 0.008	0.06

1. to demonstrate the nonlinear effects that limit the elimination of the Herzberg bands if their spectral structure is not resolved and
2. to give a solution to this problem.

In order to calculate the model spectra, the following steps were taken. Cross sections (Voigt profiles) for ro-vibronic transitions were calculated using the integrated absorption cross sections from (Yoshino *et al.*, 1995) with a Doppler width of 0.086 cm^{-1} (0.54 pm) (Yoshino *et al.*, 1994) and a Lorentz width of 0.1 cm^{-1} (0.63 pm) to obtain the measured line width at atmospheric pressure of 0.15 cm^{-1} (0.94 pm) (Yoshino *et al.*, 1994). The resulting cross section spectrum was used to calculate absorption spectra for three column densities of oxygen. The column densities were chosen to differ by a constant value and are equivalent to a groundlevel path length in the atmosphere of 240, 720 and 1200 m. Additionally, the effect of density variations with changes of atmospheric temperature and pressure was simulated for the 720 m spectrum by varying this path length by 10% (792 m, equivalent to $\Delta T = -30^\circ\text{C}$). Subsequently, these spectra were convoluted with a gaussian shaped instrument function of (1) 0.15 nm FWHM and (2) 0.05 nm FWHM, in order to (1) adjust them to a resolution comparable to atmospheric DOAS measurements and (2) study the influence of resolution on the nonlinearity. The results for the first three path lengths are shown as optical densities in Fig. 6.II for the 0.15 nm resolved spectra. As it can be seen in Fig. 6.I, individual ro-vibronic transitions are not resolved and appear as *Q*-branches in the spectrum, with 7–20 lines contributing to a “measured” absorption band. As a consequence, apparent deviations from Lambert–Beer’s law are observed in three ways: First, the observed optical density of a particular absorption band no longer depends linearly on the column density of oxygen. This complicates the correction of several absorption features of different size present in a measured spectrum. A single reference spectrum taken at a different column density then cannot be scaled linearly to eliminate both, “weak” and “strong” absorptions in a measured spectrum at the same time. As a consequence, residual structures remain. Second, the shape of a measured absorption feature will be

dependent on the column density of oxygen. A linearly scaled reference (of different $C \cdot L$) thereby will introduce additional features to the residual, i.e. will be narrower than the respective absorption band. These effects of unresolved bands generally limit the linear range of DOAS measurements (Mellqvist and Rosén, 1996) but are of special importance for the correction of the Herzberg bands since at atmospheric path lengths of a few hundred meters, the stronger lines of the Herzberg I bands ($\sigma \leq 1.6 \times 10^{-22} \text{ cm}^2$) become saturated. Third, the absorption features of O_2 may influence the apparent absorption features of another atmospheric absorber, e.g. aromatic hydrocarbon, at long path lengths if spectral features of both species overlap and are measured at ‘low’ resolution. Hence, further residual structures may result from an incomplete correction of the absorption features of the atmospheric absorber in a way similar to the so-called “solar I_0 -effect” (Johnston, 1996; Platt *et al.*, 1997).

The nonlinearity of the increasing absorption features can already be seen in Fig. 6.II, as the vertical spacing between the spectra (a) and (b) is larger than that between the spectra (b) and (c). This becomes more obvious when the absorptions of spectrum (c) are normalized to fit the band of spectrum (a) near 260.5 nm, as was done for the dashed line, indicated (c_{norm}) in Fig. 6.II. The change in the relative strength of the bands is clearly visible. The first two effects can be seen in the residual structures shown in Fig. 6.III for both resolutions (solid line: 0.15 nm, dashed line: 0.05 nm). With (d), the 720 m absorption spectrum was used to correct for the absorption features of the 1200 m spectrum. The residual (e) remains if the 720 m spectrum is used to account for typical atmospheric density variations of 10% at this path length. In case (f), two oxygen reference spectra (720 and 1200 m path length) were used simultaneously to correct for the same density variations as (e).

These results demonstrate the strong nonlinearities, that are expected from the effects of unresolved bands (residuals of a few 10^{-2}). Especially with the better resolved spectra, the change in band shape is clearly visible. For the 0.15 nm resolved spectra, residual structures were found to be half the size of the residuals from the 0.05 nm resolved spectra. This is due to

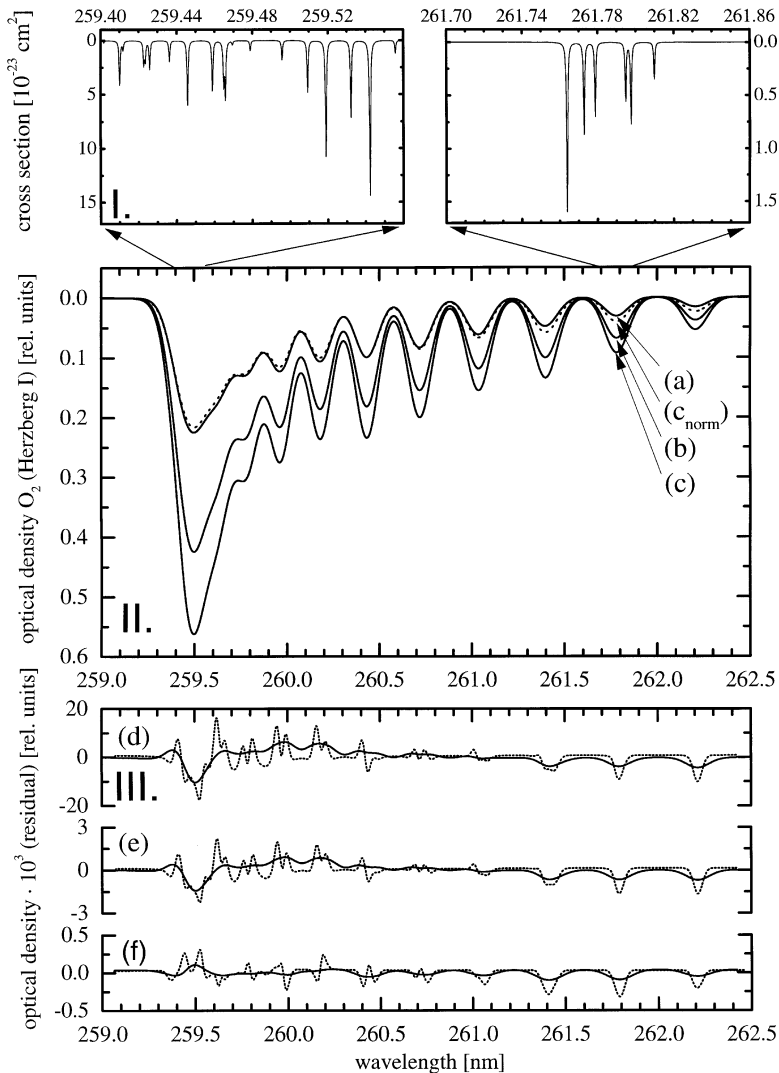


Fig. 6. Modelled cross section spectrum of the 5–0 vibronic band of the Herzberg I band system of O_2 (I shows two parts). This spectrum was used to calculate absorption spectra at different O_2 column densities and subsequently were convoluted with a gaussian shaped instrument function of 0.15 and 0.05 nm FWHM. The shown spectra (II) correspond to path lengths in the atmosphere of 240 m (a), 720 m (b) and 1200 m (c) and 0.15 nm spectral resolution. At this resolution the individual lines are not resolved and the observed shape of the spectra depends on the column density of O_2 . This is seen in the spectrum (c_{norm}) which corresponds to the spectrum (c), scaled to fit the absorption band of the spectrum (a) near 260.5 nm. Residual structures remain (d, e), if a single oxygen reference spectrum is used to correct the oxygen absorptions at a different O_2 column density, e.g. due to density variations with temperature at a fixed path length (10%). Interpolation between two oxygen reference spectra of bracketing O_2 column density allows to virtually eliminate the oxygen interference (f) (see text).

the lower optical densities that have to be corrected in this case. Density variations in O_2 , which are due to meteorological influence cause the same residual structures but reduced by roughly an order of magnitude. Nevertheless, residuals were observed to be 2.3×10^{-3} (1) and 4.5×10^{-3} (2) (see Fig. 6.III, e), respectively. It means that residual structures from incomplete correction of oxygen absorption dominate the residual spectrum, if only a single oxygen reference spectrum is fitted. If two reference spectra of bracketing O_2 column densities are scaled simultaneously

(0.15 nm resolution), the size of the residual structures can be reduced to 2×10^{-4} , i.e. a factor of five below typical detection limits. Hence, interpolation between two oxygen references allows to virtually eliminate the oxygen absorption of a “measured” spectrum that is taken at a column density in between that of the reference spectra.

3.2. Cross interference of O_2

Oxygen reference spectra at different column densities were measured as summarized in Table 3. As can

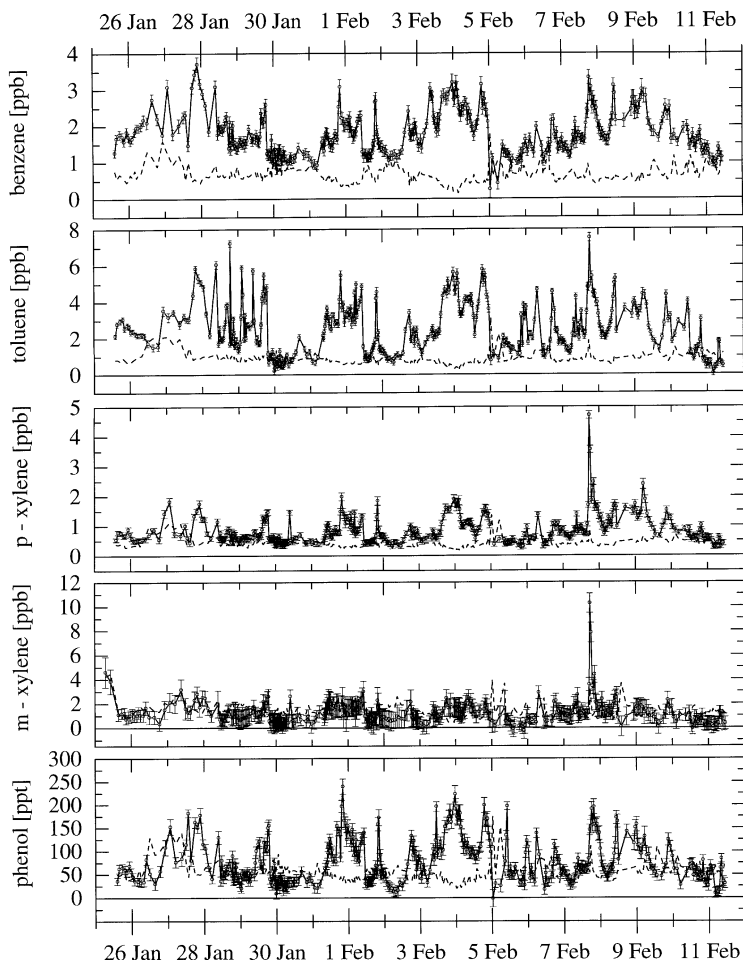


Fig. 7. Time profiles of mixing ratios of aromatic hydrocarbons measured by DOAS from 25 January 1997 until 12 February 1997 in Heidelberg, Germany. Additional with each species' mixing ratio, the respective detection limit is shown as a dashed line. Tick spacing was set to indicate days and ticks correspond to 00:00 local time.

be seen in Fig. 4 the spectra are dominated by unresolved Q -branches of the Herzberg I band system as described above and shown in the modelled spectra in Fig. 6.I. In Fig. 4 the Q -branch groupings in the vibronic bands of the Herzberg I progression are clearly visible. Observed were 10 out of 11 vibronic bands. The 0–0 band at 285.8 nm was not observed at the column densities used in the measurements. In the region between the Herzberg I vibronic band heads, i.e. at Q -branches $N \geq 17$ (N : total angular momentum apart from spin), weaker absorptions due to the Herzberg II and III bands are visible.

By adjusting a spectrum taken in 10% oxygen/90% nitrogen to one taken in 80% oxygen/20% nitrogen, band positions and bandwidths of the dimer absorption below 267 nm could be determined. These spectra cannot be used as dimer reference spectra since residual structures due to the unresolved molecular absorption (see Section 3.1) superimpose with the dimer absorption. Nevertheless, the observed dimer band positions were found in good agreement

with the positions published by Finkelnburg and Steiner (1932). From the observed width of the dimer's absorption structures the cut off of the high pass filter could be chosen to almost eliminate the dimer absorption features.

No attempts were made to study the temperature dependence of the differential structure of oxygen. Even though the cross sections are expected to depend on temperature, no dependency of the residuals size on temperature was found over the temperature range from 263 to 287 K.

3.3. Atmospheric measurements

Time series of aromatic mixing ratios measured from 25 January to 11 February 1997 in the urban air of Heidelberg are given in Fig. 7 for benzene, toluene, p -xylene, m -xylene and phenol. Additionally with the mixing ratios of the species, the detection limit is shown as a dashed line (see Section 2.2). Absorption lines of benzene, toluene, p -xylene and phenol were detected almost in each spectrum, whereas m -xylene

due to its smaller cross-section was detected only occasionally. Observed mean and maximum concentrations for detected aromatic hydrocarbons are given in Table 5. The periods, lasting several days, when concentrations of aromatics were observed to be constantly elevated were found to correlate with the wind direction. For instance, from 3 until 5 February 1997 mean concentrations of benzene, toluene, *p*-xylene and phenol were 40–80% higher than their overall mean concentrations. During this period the wind came from eastern or southeastern directions, where the centre of Heidelberg and a major road are located. Peak concentrations were observed on Friday, 7 February 1997 at 18:30 local time for toluene, *p*-xylene and *m*-xylene. At this time, wind direction was constantly east. Prominent is the steep increase of all detected aromatic concentrations at this time. Simultaneously, wind speed was found to drop from about 5 m s^{-1} at 16:00 to 0.4 m s^{-1} at 19:00, nearly recovering the former value at 21:00. Hence, this peak value can be attributed to less dilution of VOCs. Variations in the detection limit, e.g. 26 until 27 January 1997 can be attributed to the poor visibility during foggy periods resulting in increased shot noise in the measured spectra. Toluene, *p*-xylene and phenol were found to show good correlations ($R > 0.8$) with the benzene concentration. Observed ratios (on a benzene basis) were 2.31 ± 0.06 for toluene, 0.56 ± 0.01 for *p*-xylene and 0.074 ± 0.004 for phenol, respectively. Additionally, diurnal variations of the aromatic concentration were observed to coincide with daily rush hours. It is therefore most probable that all species are emitted by a common source, i.e. automobile exhaust in Heidelberg.

3.3.1. Interference effects of aromatic species. At the resolution used for the measurements absorption features of individual aromatic hydrocarbons are well selective due to minimized spectral overlap of their absorption line positions and shape of their differential structure.

Reference spectra of aromatic species, measured at higher resolution ($3600 \text{ grooves mm}^{-1}$ grating, $\text{FWHM} = 50 \text{ pm}$) did not show a significant gain in differential structure. Therefore, it is not expected to greatly increase DOAS selectivity at this resolution. Nevertheless light throughput at this resolution is reduced by about an order of magnitude and thereby time resolution would be limited. At lower resolution spectral features will be lost and, as a consequence, DOAS selectivity will be reduced. Moreover the linear range (see Section 3.1) of DOAS measurements will be further decreased.

With respect to the recording of DOAS spectra, the chosen resolution (0.16 nm), therefore, is assumed to be close to an optimum resolution, yielding high sensitivity, good selectivity and a reasonable time resolution for the measurements of aromatic compounds.

Additionally, the applied high pass filters were optimized with respect to maximum signal to noise ratios for benzene, toluene, *p*-xylene and phenol as well as

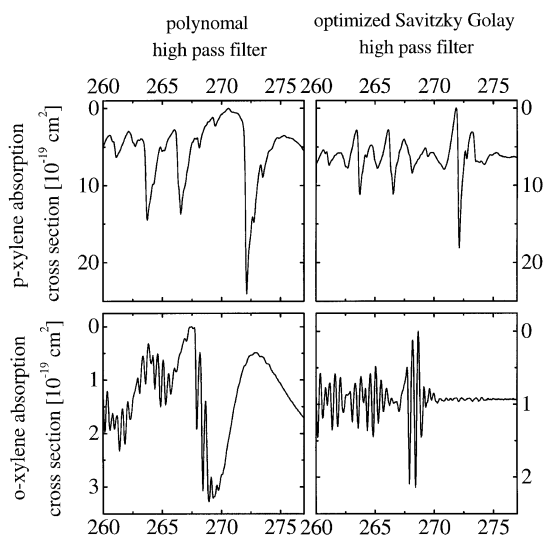


Fig. 8. Flexible high pass filters on the basis of smoothing routines allow to optimize the cut off of the filter for the species of interest. This can also be used to reduce cross sensitivities of aromatic hydrocarbons as it is shown in the example of *p*- and *o*-xylene.

m-xylene and thereby inherently minimize effects that result from negative correlations. As an example, this is demonstrated in Fig. 8 for the interference of *o*- and *p*-xylene. To reconstruct the negative correlation of the differential structures shown in (Axelsson *et al.*, 1995) a polynomial (4th order) high pass filter was used (left panels in Fig. 8). The differential cross section of *p*-xylene is 8 times larger than that of *o*-xylene and at same mixing ratios the differential absorption features of *p*-xylene will dominate in a measured spectrum. If such a spectrum is evaluated only with respect to *o*-xylene, a negative concentration will be found. On the other hand, if *o*-xylene is omitted, the *p*-xylene concentration will be underestimated (Axelsson *et al.*, 1995). By the application of an optimized Savitzky Golay high pass filter (Savitzky and Golay, 1964; Volkamer, 1996), this interference can be almost eliminated (right panels in Fig. 8) and DOAS selectivity thereby will be enhanced. As a consequence of optimized high pass filtering, the signal to noise ratio could be improved by a factor of up to 2.4 as compared to using a polynomial high-pass filter, reflecting in part a successful elimination of the dimer absorption.

Active control has to be taken of the fit parameters, i.e. spectral shifts. Especially with the detection of aromatic hydrocarbons, i.e. with those showing low absorptions close to the detection limit, spectral shifts need to be critically separated due to thermal effects and numerical artefacts. Due to the thermostated spectrometer unit, thermal shifts are expected to be less than 8×10^{-3} (corresponding to $5 \mu\text{m}$ on the diode array) for our instrument. As a consequence, no shifts were allowed for aromatic reference spectra.

With the resolution used for the measurements and the optimized high pass filter used for data evaluation, mutual interference effects for aromatic species present in the urban air of Heidelberg could almost be eliminated.

4. CONCLUSIONS AND OUTLOOK

The reference spectra presented here eliminate the interference of the Herzberg bands of oxygen with UV spectroscopic measurements of aromatic hydrocarbons for practical purposes. This was demonstrated with the application of the spectra to atmospheric DOAS measurements of aromatic species and allowed for the first time the sensitive DOAS measurement of absolute concentrations of monocyclic aromatic hydrocarbons.

For a general solution of the O₂ interference, cross sections of all the three Herzberg band systems need to be recorded at a resolution well below the line width at ambient conditions. The temperature dependence of the cross sections probably can be calculated with sufficient precision. These cross sections then could be used as "infinitely well" resolved cross section spectra and could be adjusted to the resolution of the measurements to correct the O₂ interference (by convoluting them with the instrument function) for any O₂ column density. Measurements at room temperature are presently carried out by Carleer *et al.* (1996).

In addition, a digitized reference spectrum of the dimer absorption needs to be taken.

Furthermore, no measurements of monocyclic aromatic cross sections at a resolution better than 50 pm (FWHM) are known. If rotational transitions of the aromatic species were resolved, as it was shown for naphthalene (Neuroth *et al.*, 1991), DOAS selectivity could be further enhanced.

Acknowledgements—Material support by the BASF, Ludwigshafen, Germany is gratefully acknowledged. The authors would further like to thank Prof. Ulrich Schurath for his very helpful comments on the manuscript.

REFERENCES

Amoruso, A., Crescentini, L., Cola, M. and Fiocco, G. (1996) Oxygen absorption cross-section in the Herzberg continuum. *Journal of Quantitative Spectroscopy and Radiative Transfer* **56**, 145–152.

Atkinson, R. (1994) Gas-phase tropospheric chemistry of organic compounds. *Journal of Physical Chemical Reference Data Monograph No. 2*, 1–216.

Axelsson, H., Eilard, A., Emanuelsson, A., Galle, B., Edner, H., Ragnarson, P. and Kloo, H. (1995) Measurement of aromatic hydrocarbons with the DOAS technique. *Applied Spectroscopy* **49**, 1254–1260.

Bao, Z., Yu, W. and Barker, J. (1995) Absolute integrated cross sections for some O₂ Herzberg I transitions near 248–249 nm. *Journal of Chemical Physics* **103**, 6–13.

Barrefors, G. (1996) Monitoring of benzene, toluene and p-xylene in urban air with differential optical absorption

spectroscopy technique. *Science of the Total Environment* **189/190**, 287–292.

Bass, A. and Paur, R. (1985) The ultraviolet cross section of ozone, I. The measurements. In: (eds) Z. C. and A. Ghazy, *Proceedings of the Quadrennial Ozone Symposium*, Chalkidiki, Greece, pp. 606–616.

Becker, K. (1994) The atmospheric oxidation of aromatic hydrocarbons and its impact on photooxidant chemistry. *Proceedings of EUROTRAC Symposium, Transport and Transformation of Pollutants in the Troposphere*, eds. P. M. Borrell *et al.*, pp. 67–74. *SPB Academic Publishing, The Hague*.

Blake, A. and McCoy, D. (1987) The pressure dependence of the Herzberg photoabsorption continuum of oxygen. *Journal of Quantitative Spectroscopy and Radiative Transfer* **38**, 113–120.

Blake, D., Smith, T., Chen, T.-Y., Whipple, W. and Rowland, F. (1994) Effects of biomass burning on summertime non-methane hydrocarbon concentration in the Canadian wetlands. *Journal of Geophysical Research* **99**, 1699.

Borrell, P., Borrell, P. and Ramsay, D. (1986) High-resolution studies of the near-ultraviolet bands of oxygen: II: The A³Σ_u⁻ ← X³Σ_g⁻ system. *Canadian Journal of Physics* **64**, 721–725.

Brocco, D., Fratascangeli, R., Lepore, L., Petricca, M. and Ventrone, I. (1997) Determination of aromatic hydrocarbons in urban air of rome. *Atmospheric Environment* **31**, 557–566.

Carleer, M., Fally, S., Colin, R., Jenouvrier, A., Mérienne, M., Hermans, C., Vandaele, A. and Simon, P. (1996) O₂ absorption cross-sections and absolute intensities in the UV-visible using a fourier transform spectrometer. In *Workshop on Atmospheric Spectroscopy Applications, 'ASA Reims 96'*, University de Reims Champagne Ardenne, France, 4–6 September 1996.

Conner, T. and Stevens, R. (1991) Air quality monitoring in atlanta with the differential optical absorption spectrometer. *84th Annual Meeting of Air and Waste Management Association*, Vancouver.

Coquart, B. and Ramsay, D. A. (1986) High-resolution studies of the near-ultraviolet bands of oxygen: III: The A³Δ_u ← X³Σ_g⁻ system. *Canadian Journal of Physics* **64**, 726–732.

Derwent, R., Jenkin, M. and Saunders, S. (1996) Photochemical ozone creation potentials for a large number of reactive hydrocarbons under european conditions. *Atmospheric Environment* **30**, 181–199.

Dewulf, J., Ponnet, D. and Vanlangenhove, H. (1996) Measurement of atmospheric monocyclic aromatic hydrocarbons and chlorinated C-1-hydrocarbons and C-2-hydrocarbons at ng m⁻³ concentration level. *International Journal of Environmental Analytical Chemistry* **62**, 289–301.

Dewulf, J. and Langenhove, H. (1997) Analytical techniques for the determination and measurement data of 7 chlorinated C₁- and C₂- hydrocarbons and 6 monocyclic aromatic hydrocarbons in remote air masses: an overview. *Atmospheric Environment* **31**, 3291–3307.

Dianov-Klokov, V. (1966a) Absorption by gaseous oxygen and its mixtures with nitrogen in the 2800–2350 Å range. *Optics and Spectroscopy* **21**, 233.

Dianov-Klokov, V. (1966b) Absorption spectrum of condensed oxygen in the 1.26–0.3 μm region. *Optics and Spectroscopy* **20**, 530–534.

Ditchburn, R. and Young, P. (1962) The absorption of molecular oxygen between 1850 and 2500 Å. *Journal of Atmospheric Terrestrial Physics* **24**, 127–130.

Eitzer, B. (1995) Emission of volatile organic chemicals from municipal solid waste composting facilities. *Environmental Science and Technology* **29**, 896–902.

England, J., Lewis, B. and Gibson, S. (1996) Electronic transition moments for the Herzberg I bands of O₂. *Canadian Journal of Physics* **74**, 185–193.

- Epifanov, S. and Vigin, A. (1994) Contribution of bound, metastable and free states of bimolecular complexes to collision-induced intensity of absorption. *Chemical Physics Letters* **225**, 537–541.
- Etzkorn, T. (1998) Dissertation, Institut fuer Umweltp Physik, University of Heidelberg.
- Etzkorn, T., Klotz, B., Sørensen, S., Patroescu, I., Barnes, I., Becker, K. and Platt, U. (1998) Gas-phase absorption cross sections of 24 monocyclic aromatic hydrocarbons in the UV and IR spectral ranges. *Atmospheric Environment* (submitted).
- Eyde, L. and Richards, G. (1991) Analysis from wood smoke: components derived from polysaccharides and lignins. *Environmental Science and Technology* **25**, 1133–1137.
- Fateley, W., Hammaker, R., Tucker, M., Witkowski, M., Chaffin, C., Marshall, T., Davis, M., Thomas, M. J., Arelló, J., Hudson, J. and Fairless, B. (1995) Observing industrial atmospheric environments by FT-IR. *Journal of Molecular Structure* **347**, 153–168.
- Finkelburg, W. and Steiner, W. (1932) Ueber die absorptionsspektren des hochkomprimierten sauerstoffs und die existenz von O₄ molekülen I. die ultravioletten banden zwischen 2900 und 2300 Å. *Zeitschrift für Physik* **79**, 69–88.
- Franzen, J., Frey, R. and Nagel, H. (1995) Fast monitoring of motor exhaust compounds by resonant multi-photon ionisation and time-of-flight mass spectrometry. *Journal of Molecular Structure* **347**, 143–152.
- Gomer, T., Brauers, T., Heintz, F., Stutz, J. and Platt, U. (1993) *MFC User Manual, Vers. 1.98*. Institut fuer Umweltp Physik, University of Heidelberg.
- Greenberg, J., Lee, B., Helmig, D. and Zimmermann, P. (1994) Fully automated gas chromatograph-flame ionization detector system for the in situ determination of atmospheric non-methane hydrocarbons at low parts per trillion concentration. *Journal of Chromatography A* **676**, 389–398.
- Greenblatt, G. D., Orlando, J. J., Burkholder, J. B. and Ravishankara, A. R. (1990) Absorption measurements of oxygen between 330 and 1140 nm. *Journal of Geophysical Research* **95**, 18,577–18,582.
- Hasson, V. and Nicholls, R. (1971) Absolute spectral absorption measurements on molecular oxygen from 2640–1929 Å: I. Herzberg I (³Σ⁺ – ³Σ⁻) bands (2640–2430 Å). *Journal of Physics B: Atomic and Molecular Physics* **4**, 1778.
- Helmig, D. and Greenberg, J. (1994) Automated in situ gas chromatographic-mass spectrometric analysis of ppt level volatile organic trace gases using multistage solid-adsorbent trapping. *Journal of Chromatography A* **677**, 123–132.
- Herzberg, G. (1932) *Naturwissenschaften* **20**, 577.
- Herzberg, G. (1952) Forbidden transitions in diatomic molecules II: The ³Σ_u⁺ ← ³Σ_g⁻ absorption bands of the oxygen molecule. *Canadian Journal of Physics* **30**, 185.
- Horowitz, A., Schneider, W. and Moortgat, G. (1989) The role of oxygen dimer in oxygen photolysis in the Herzberg continuum. A temperature dependence study. *Journal of Physical Chemistry* **93**, 7859–7863.
- Huestis, D., Copeland, R., Knutsen, K., Slinger, T., Jongma, R., Boogaarts, M. and Meijer, G. (1994) Branch intensities and oscillator strengths for the Herzberg absorption system in oxygen. *Canadian Journal of Physics* **72**, 1109–1121.
- Hunt, J., Miller, R. and Whelan, J. (1980) Formation of C₄–C₇ hydrocarbons from bacterial degradation of naturally occurring terpenoids. *Nature* **288**, 577–578.
- Ioffe, B., Isidorov, V. and Zenkevich, I. (1979) Certain regularities in the composition of volatile organic pollutants in the urban atmosphere. *Environmental Science and Technology* **13**, 864–868.
- Isidorov, V., Zenkevich, I. and Ioffe, B. (1990) Volatile organic compounds in solfatoric gases. *Journal of Atmospheric Chemistry* **10**, 329.
- Johnston, H., Paige, M. and Yao, F. (1984) Oxygen absorption cross sections in the Herzberg continuum. *Journal of Geophysical Research* **89**, 11,661–11,665.
- Johnston, P. (1996) Unpublished manuscript.
- Juettner, F. and Henatsch, J. (1986) Anoxic hypolimnion is a significant source of biogenic toluene. *Nature* **323**, 797–798.
- Kerr, C. and Watson, J. (1986) *Canadian Journal of Physics* **64**, 36.
- Loefgren, L. (1992) Determination of benzene and toluene in urban air with differential optical absorption spectroscopy. *International Journal of Environmental Analytical Chemistry* **47**, 69–74.
- Martin-Revejo, M., Pons, M., Wirtz, K., Etzkorn, T. and Senzig, J. (1996) An outdoor smog chamber study of the gas-phase chemistry of toluene and xylenes in NO_x/air systems. In: *7th European Symposium on Physico-Chemical Behavior of Atmospheric Pollutants*, Venedig, 30th November – 4th October 1996.
- Mellqvist, J. and Rosén, A. (1996) DOAS for flue gas monitoring - II. deviations from the Beer–Lambert law for the UV/visible absorption spectra of NO, NO₂, SO₂ and NH₃. *Journal of Quantitative Spectroscopy and Radiative Transfer* **56**, 209–224.
- Miller, R., Suits, A., Houson, P., Toumi, R., Mach, J. and Wodtke, A. (1994) The Ozone deficit problem: O₂ (X, v = 26) + O (³P) from 226-nm ozone photodissociation. *Science* **265**, 1831–1838.
- Milton, M., Woods, P., Jolliffe, B., Swann, N. and McIveen, N. (1992) Measurements of toluene and other aromatic hydrocarbons by differential-absorption LIDAR in the near-ultraviolet. *Applied Physics B* **55**, 41–45.
- Neuroth, R., Dorn, H.-P. and Platt, U. (1991) High resolution spectral features of a series of aromatic hydrocarbons and BrO: potential interferences in atmospheric OH-measurements. *Journal of Atmospheric Chemistry* **12**, 287–298.
- Nutmagul, W. and Cronn, D. (1985) Determination of selected aromatic hydrocarbons at remote continental and oceanic locations using photoionization/flame-ionisation detection. *Journal of Atmospheric Chemistry* **2**, 415–433.
- Odom, J., Jungkamp, T., Griffin, R., Flagan, R. and Seinfeld, J. (1997) The atmospheric aerosol-forming potential of whole gasoline vapor. *Science* **276**, 96–99.
- Orlando, J., Tyndall, G., Nickerson, K. and Calvert, J. (1991) The temperature dependence of collision-induced absorption by oxygen near 6 μm. *Journal of Geophysical Research* **96**, 20,755–20,760.
- Ottobri, B., Guerra, A. N., Saeger, E. D. and Sandroni, S. (1996) Validation of a DOAS instrument for the measurement of atmospheric trace constituents. *EUR Report 16413 EN*.
- Partridge, R., Curtis, I. H., Goody, B. and Woods, P. (1995) An evaluation of the performance of an open-path atmospheric air-quality monitor manufactured by OPSIS, Sweden. *NPL Report Qu109*.
- Penkett, S. (1993) The tropospheric chemistry of ozone in the polar regions. In: *Measurements of Hydrocarbons in Polar Maritime Air Masses*, ed. B. Niki Springer, Berlin.
- Perner, D. and Platt, U. (1980) Absorption of light in the atmosphere by collision pairs of oxygen (O₂)₂. *Geophysical Research Letters* **7**, 1053–1056.
- Perry, R. and Gee, I. (1994) Vehicle emissions in relation to fuel composition. In *Proceedings of the 3rd International Symposium on Transport and Air Pollution*, Avignon, p. 129.
- Piccot, S., Watson, J. and Jones, J. (1992) A global inventory of volatile organic compound emissions from anthropogenic sources. *Journal of Geophysical Research* **97**, 9897–9912.
- Pitts, J., Biermann, H., Winer, A. and Tuazon, E. (1984) Spectroscopic identification and measurement of gaseous nitrous acid in dilute auto exhaust. *Atmospheric Environment* **18**, 847–854.

- Platt, U. (1994) Differential optical absorption spectroscopy (DOAS). In: *Monitoring by Spectroscopic Techniques*, ed. M. W. Sigrist, Wiley, New York.
- Platt, U., LeBras, G., Poulet, G., Burrows, J. and Moortgat, G. (1990) Peroxy radical from night-time reaction of NO₃ with organic compounds. *Nature* **348**, 147–149.
- Platt, U., Marquard, L., Wagner, T. and Perner, D. (1997) Corrections for zenith scattered light DOAS. *Geophysical Research Letters* **24**, 1759–1762.
- Platt, U. and Perner, D. (1983) Measurements of atmospheric trace gases by long path differential UV/visible absorption spectroscopy. In: *Optical and Laser Remote Sensing*, eds. D. Killinger and A. Mooradian, pp. 95–105. Springer, New York.
- Ramsay, D. (1986) High-resolution studies of the near-ultraviolet bands of oxygen: I: The $c^1\Sigma_u^- \leftarrow X^3\Sigma_g^-$ system. *Canadian Journal of Physics* **64**, 717–720.
- Ritz, D., Hausmann, M. and Platt, U. (1992) An improved open path multi-reflection cell for the measurement of NO₂ and NO₃. *Optical Methods in Atmospheric Chemistry* **1715**, 200–211.
- Rudolf, J., Johnen, F. and Khedim, A. (1986) Problems connected with the analysis of halocarbons and hydrocarbons in the non-urban atmosphere. *International Journal of Environmental Analytical Chemistry* **27**, 97–122.
- Sack, T., Steele, D., Hammerstrom, K. and Remmers, J. (1992) A survey of household products for volatile organic compounds. *Atmospheric Environment* **26A**, 1063.
- Sandroni, S., Cerutti, C., Noriega, A. and Palmgren, F. (1994) Air quality measurements in brussels. *EUR Report* 16091 EN.
- Savitzky, A. and Golay, M. (1964) Smoothing and differentiation of data by simplified least squares procedures. *Analytical Chemistry* **36**, 1627–1639.
- Shardanand (1969) Absorption cross sections of O₂ and O₄ between 2000 and 2800 Å. *Physical Review* **186**, 5–9.
- Shardanand (1977) Nitrogen-induced absorption of oxygen in the Herzberg continuum. *Journal of Quantitative Spectroscopy and Radiative Transfer* **18**, 525–530.
- Stutz, J. and Platt, U. (1992) Problems in using diode arrays for open path DOAS measurements of atmospheric species. *Proc. EOS/SPIE Symp. Berlin, Optical Methods in the Atmospheric Chemistry* **1715**, 329–340.
- Stutz, J. and Platt, U. (1996) Numerical analysis and estimation of the statistical error of differential optical absorption spectroscopy measurements with least-squares methods. *Applied Optics* **35**, 6041–6053.
- Stutz, J. and Platt, U. (1997) Improving long-path differential optical absorption spectroscopy with a quartz fiber mode mixer. *Applied Optics* **36**, 1105–1115.
- Trankovsky, E., Ben-Shalom, A., Oppenheim, U., Devir, A., Balfour, L. and Engel, M. (1989) Contribution of oxygen to attenuation in the solar blind UV spectral region. *Applied Optics* **28**, 1588–1591.
- Trost, B. (1997) UV-absorption cross sections of a series of monocyclic aromatic compounds. *Atmospheric Environment* **31**, 3999–4008.
- Vandaele, A., Simon, T., Goumout, J., Carleer, C. and Colin, R. (1994) SO₂ absorption cross section measurement in the UV using fourier transform spectrometer. *Journal of Geophysical Research* **99**, 25,599–25,605.
- Volkamer, R. (1996) Absorption von sauerstoff im Herzberg I system und anwendung auf aromatenmessungen am EUROpean PHOtO REactor (EUPHORE). Diploma Thesis, Institut fuer Umweltp Physik, University of Heidelberg.
- Warburg, E. (1915) Ueber den energieumsatz bei photochemischen vorgaengen in gasen: V. absorption ultravioletter strahlung durch sauerstoff. *Sitzungsber. d. Preuß. Akad. D. Wiss.*, **230**.
- Weitkamp, C., Goers, U. B., Glauer, J., Koehhler, S., Rairoux, P., Immler, F., Woeste, L., Ulbricht, M. and Weidauer, D. (1996) Laser remote sensing of sulfur dioxide, nitrogen dioxide, toluene, ozone and dust in the industrial aera of Cubatao (Brazil). In: *Advances in Atmospheric Remote Sensing with Lidar*, eds. A. Ansmann, R. Neuber, P. Rairoux and U. Wandinger, *Selected papers of the 18th ILRC*, Berlin 22–26 July 1996, pp. 411. Springer, Heidelberg.
- Westerholm, R., Almen, J., Li, H., Rannug, U. and Rosen, A. (1992) Exhaust emissions from gasoline-fuelled light duty vehicles operated in different driving conditions: a chemical and biological characterization. *Atmospheric Environment* **26B**, 79.
- White, J. (1976) Very long optical paths in air. *Journal of Optical Society of America* **66**, 411–416.
- Wilkerson, T., Fraize, W. and Price, B. (1992) Long-path UV spectroscopic and in situ measurements of air pollutants in the Washington DC and middle Atlantic regions. *Optical Methods in Atmospheric Chemistry* **1715**, 267–285.
- Wulf, O. (1928) Photochemical ozonization and its relation to the polymerization of oxygen. *Proceedings of the National Academy of America* **14**, 356.
- Yoshino, K., Esmond, J., Murray, J., Parkinson, W., Thorne, A., Learner, R. and Cox, G. (1995) Band oscillator strengths of the Herzberg I bands of O₂. *Journal of Chemical Physics* **103**, 1243–1249.
- Yoshino, K., Murray, J., Esmond, J., Sun, Y., Parkinson, W., Thorne, A., Learner, R. and Cox, G. (1994) Fourier transform spectroscopy of the Herzberg I bands of O₂. *Canadian Journal of Physics* **72**, 1101–1108.